Metallomics

Accepted Manuscript

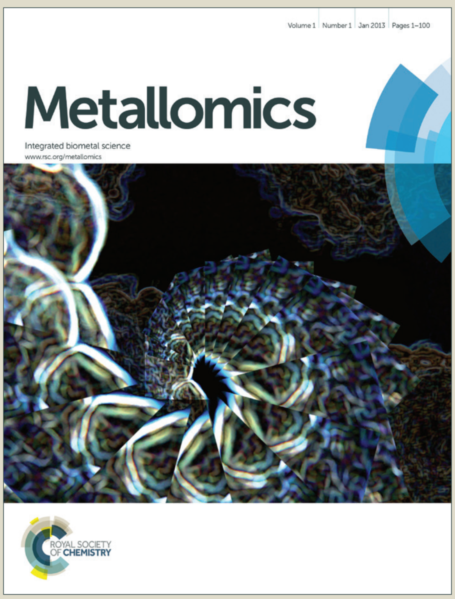

This is an *Accepted Manuscript*, which has been through the Royal Society of Chemistry peer review process and has been accepted for publication.

Accepted Manuscripts are published online shortly after acceptance, before technical editing, formatting and proof reading. Using this free service, authors can make their results available to the community, in citable form, before we publish the edited article. We will replace this *Accepted Manuscript* with the edited and formatted *Advance Article* as soon as it is available.

You can find more information about *Accepted Manuscripts* in the Information for Authors.

Please note that technical editing may introduce minor changes to the text and/or graphics, which may alter content. The journal's standard Terms & Conditions and the Ethical guidelines still apply. In no event shall the Royal Society of Chemistry be held responsible for any errors or omissions in this *Accepted Manuscript* or any consequences arising from the use of any information it contains.

ROYAL SOCIETY OF CHEMISTRY

www.rsc.org/metallomics

To be submitted to *Metallomics*

Biological effect of nitroimidazole derivative of polypyridyl ruthenium complex on cancer and endothelial cells

Olga Mazuryk[a], Franck Suzenet[b], Claudine Kieda[c, *], Małgorzata Brindell[a,*]

[a] *Department of Inorganic Chemistry, Faculty of Chemistry, Jagiellonian University, Ingardena 3, 30-060 Krakow, Poland*

[b] *Institute of Organic and Analytical Chemistry, University of Orléans, UMR-CNRS 7311, rue de Chartres, BP 6759, 45067 Orléans Cedex 2, France*

[c] *Centre de biophysique moléculaire, CNRS, rue Charles Sadron, 45071, Orléans Cedex 2, France*

Corresponding Authors

*M. B. e-mail: brindell@chemia.uj.edu.pl phone: (+48) 12 663 22 21.

*C. K. e-mail: claudine.kieda@cnrs-orleans.fr phone: (+33) 238 25 55 61.

† Electronic supplementary information (ESI) available: Additional figures illustrating accumulation/uptake data, mRNA expression of several genes.

ABSTRACT

The ruthenium polypyridyl complexes $[Ru(dip)_2(bpy/bpy\text{-}2\text{-}nitroIm)]^{2+}$ (dip = 4,7-diphenyl-1,10-phenanthroline, bpy = 2,2'-bipyridine, bpy-2-nitroIm = 4-[3-(2-nitro-1*H*-imidazol-1-yl)propyl]) were found to be ca. ten times more cytotoxic against breast cancer (4T1) and human lung adenocarcinoma epithelial cells (A549) than a well-known anticancer drug cisplatin. Even though the Ru complexes were quite cytotoxic towards FVB mouse lung microvascular endothelial cells (MLuMEC FVB) their efflux from these non transformed cells was much more efficient than from cancer ones. Both Ru complexes were accumulating

Metallomics Accepted Manuscript

in cells. The cellular uptake of both Ru complexes occurs through passive diffusion while nitroimidazole derivative is also endocytosed. They arrest cell growth in S-phase and induce apoptosis. Such cell response can result from activation of oxidative stress by Ru complexes. The modulation of mRNA expression profile for genes which might be involved in metastasis and angiogenesis processes by Ru complexes was analyzed for both cancer (4T1) and endothelial (MLuMEC FVB) cells. Ru complexes appeared to have a distinct impact on cell adhesion and migration as well as they effect on endothelial cells vasculature. They are not only cytotoxic but are potential invasive and anti-metastasic agents. The work illustrates the putative future development of polypyridyl ruthenium.

INTRODUCTION

During the last decade a growing interest in applications of Ru polypyridyl complexes as luminescent dyes for optical imaging or as cytotoxic agents for the treatment of various types of cancer has been observed.[1-10] Even though the biological activity of many Ru polypyridyl complexes has been actively investigated there is still little information about the mechanism of action of this class of compounds. Many efforts have been made to design compounds which target nucleic acids in cell,[11] and very interesting results concerning probing DNA mismatches *in vitro* have been recently obtained.[12] However many of the studied Ru complexes which presented good intercalating properties for isolated DNA, were not able to cross the complex milieu surrounding the cell nucleus to reach the polynucleotide chain to interact with. In contrast, very little attention has been paid to their interaction with proteins, which might represent quite crucial alternative as targets for this type of complexes. By influencing protein structure they can change significantly their reactivity. The future success in the design of effective optical probes for imaging or cytotoxic agents based on

Metallomics Accepted Manuscript

polypyridyl Ru complexes depends greatly on understanding their mode of action and the identification of their molecular targets.

Very recently we have designed a new Ru polypyridyl complex comprising nitroimidazole unit $[Ru(dip)_2(bpy\text{-}2\text{-}nitroIm)]Cl_2$ (dip is 4,7-diphenyl-1,10-phenanthroline, bpy-2-nitroIm is 4-[3-(2-nitro-1*H*-imidazol-1-yl)propyl], Scheme 1) in the purpose of targeting hypoxic cells.[13] It is believed that upon irreversible (under hypoxic conditions) reduction of a nitroimidazole moiety the formed derivatives can further interact with proteins and/or DNA and the compound is trapped inside cells.[13, 14] The preliminary biological studies have pointed out its fast and efficient accumulation inside the cells and a relatively high cytotoxicity. These properties were enhanced in hypoxic conditions, which was not observed for $[Ru(dip)_2(bpy)]Cl_2$. In this paper we show the influence of various parameters on the antiproliferative activity of both compounds against cancer and endothelial cells, and describe the rules that govern their cellular uptake as well as their pro-apoptotic and cell-cycle arresting properties. To better understand how these Ru polypyridyl complexes can influence the cell behavior we have checked their ability to alter cell adhesion and mobility. Inhibition of these two processes in tumor cells is one of the aims of anti-metastatic treatments.[15] Another important feature which can contribute to anti-metastatic effects, induced by anticancer agents is their influence on the angiogenesis process.[16] Antitumor and particularly, anti-metastatic effects, are often related to an anti-angiogenic effect.[17] Tumor angiogenesis is a complex process of response to hypoxia and results in the formation of incomplete, leaky, permeable vessels, inefficiently supplying oxygen and nutrients to tumors cells.[18] Nevertheless, a complete shutdown of angiogenesis often leads to the selection of more aggressive, drug resistant stem-like cancer cells.[18] If the tumor is not well perfused, chemotherapeutics do not have an access to cancer cells. Furthermore, one of the adaptive mechanism of hypoxic cells is to slow down their growth rate which reduces the toxicity of

Metallomics Accepted Manuscript

most chemotherapeutic drugs.[19] Normalization of angiogenesis is a proven powerful adjuvant strategy for cancer treatment.[18] To get closer to the molecular mechanism underlying the observed biological effects, the influence of both complexes on mRNA expression of several genes was analyzed. Among others the level of matrix metalloproteinase (MMP) genes expression was addressed. Indeed, as tumor cells have to pass through the extracellular matrix and several layers of different tissues in order to intravasate and metastasize, they frequently overexpress MMPs.[20] Taken together these biological approaches bring a new insight into the properties and applications of Ru polypyridyl class of complexes.

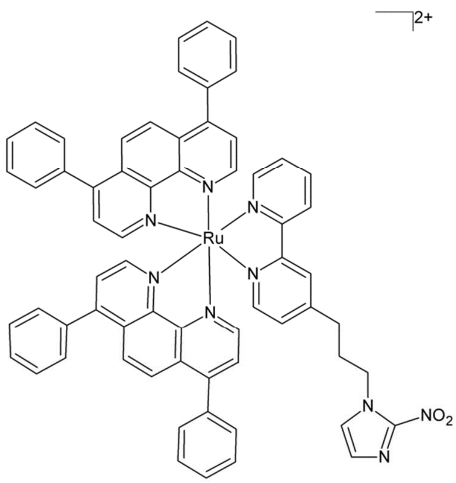

Scheme 1. $[Ru(dip)_2(bpy\text{-}2\text{-}nitroIm)]^{2+}$

RESULTS AND DISCUSSION

Cytotoxicity of Ru complexes *in vitro*

The cytotoxic effect of $[Ru(dip)_2(bpy\text{-}NitroIm)]^{2+}$ and $[Ru(dip)_2(bpy)]^{2+}$ was determined on two cancer cell lines: murine mammary carcinoma (4T1) and human lung adenocarcinoma cell line (A549). In addition, antiproliferative activity was assessed for mature (MLuMEC) and precursor (MAgEC 10.5) endothelial cells.[21, 22] 4T1, MLuMEC and

Metallomics Accepted Manuscript

MAgEC 10.5 cells come from the same species and allow for studying the influence of the investigated Ru complexes on cancerous and non-transformed cells. A549 cells were additionally included into this study since unlike 4T1 cells they express nitroreductase (reported in this study), the enzyme which might be engaged in conversion of nitroimidazole moiety. This process can have a distinct impact on mode of action of the $[Ru(dip)_2(bpy\text{-}NitroIm)]^{2+}$, in particular under hypoxic conditions.[13, 23] Cisplatin was used as a control. The studies included the influences of serum (2%), incubation time and hypoxic conditions on cytotoxic activity. All studied complexes exhibited a dose-dependent growth inhibitory effect on all tested cell lines. The IC_{50} values of Ru complexes and cisplatin are listed in Table 1.

Table 1. IC_{50} of $[Ru(dip)_2(bpy\text{-}NitroIm)]^{2+}$, $[Ru(dip)_2(bpy)]^{2+}$ and cisplatin against selected cell lines. Experiments were performed in medium without (S−) or with (S+, 2%) serum.

Metallomics Accepted Manuscript

To be submitted to *Metallomics*

	IC_{50} [μM]	Normoxia				Hypoxia			
		24 h		48 h		24 h		48 h	
		S-	S+	S-	S+	S-	S+	S-	S+
$[Ru(dip)_2(bpy\text{-}NitroIm)]Cl_2$	MAgEC 10.5	4.7±0.6	7.4±0.8	4.6±0.3	8.1±2.4	7.5±0.6	7.1±1.0	2.3±0.3	7.1±1.2
	MLuMEC FVB	6.1±0.7	10.4±1.3	6.9±1.0	15.0±4.2	4.9±1.1	13.4±1.3	4.9±1.4	11.2±1.7
	4T1	10.6±1.1	18.8±1.3	5.9±0.8	8.7±0.9	7.1±0.5	12.3±2.2	8.3±1.0	7.3±1.9
	A549	11.8±1.2	17.5±5.7	1.5±0.2	3.4±0.5	7.7±0.4	10.9±2.8	3.7±0.2	4.9±1.6
$[Ru(dip)_2(bpy)]Cl_2$	MAgEC 10.5	3.1±0.3	4.9±0.8	3.3±0.1	11.7±1.0	2.1±0.3	4.4±1.3	2.5±0.2	4.1±0.4
	MLuMEC FVB	4.7±0.4	11.7±1.6	4.2±0.6	16.7±1.9	4.3±0.4	9.4±0.9	2.2±0.3	4.3±0.7
	4T1	6.8±1.1	13.6±1.8	6.4±0.5	11.9±1.4	6.8±1.3	8.7±1.3	4.6±0.3	5.2±0.9
	A549	13.5±5.3	27.7±1.2	2.2±0.2	4.8±0.2	4.7±0.8	5.9±0.3	0.9±0.1	4.7±0.9
cisplatin	MAgEC 10.5	9.4±0.7	8.8±0.2	3.6±0.2	2.7±0.2	7.6±1.1	6.5±0.4	3.2±0.3	3.0±0.1
	MLuMEC FVB	24.6±2.9	14.5±1.4	11.1±0.6	6.7±0.5	29.0±4.3	18.9±1.2	12.5±1.0	8.0±0.6
	4T1	73.0±14.9	59.8±8.3	11.2±0.3	7.6±2.7	52.5±4.9	43.0±4.7	13.6±1.3	15.2±3.1
	A549	126.0±31	71.3±23	79.9±5.3	47.4±32	-	-	-	-

Metallomics Accepted Manuscript

$[Ru(dip)_2(bpy\text{-}NitroIm)]^{2+}$ strongly inhibited growth of tested cell lines with IC_{50} ranging from 1.5 to 18.8 μM. Under the same conditions cisplatin was found to be less cytotoxic than tested Ru compounds, particularly for cancer cell lines 4T1 and A549. Comparison of the IC_{50} values for $[Ru(dip)_2(bpy\text{-}NitroIm)]^{2+}$ and $[Ru(dip)_2(bpy)]^{2+}$, points out that the addition of nitroimidazole moiety to the Ru complex slightly decreased its cytotoxic effect probably due to its slower/lower accumulation. Since endothelial cells are about 10-100 times more susceptible to chemotherapeutic agents than cancer cells,[24] it was expectable that precursor endothelial cells MAgEC 10.5 and mature endothelial cells MLuMEC FVB would be more sensitive to the Ru compounds and to cisplatin, but cancer cell lines 4T1 and A549 were only slightly less susceptible to both Ru complexes.

The duration of incubation did not influence greatly the antiproliferative effect of both Ru complexes, indicating that they exert their cytotoxic activity within a short delay as previously observed.[13] The presence of serum in the incubation medium decreases the cytotoxic activity of the Ru complexes. The medium effect might arise from the formation of Ru-protein adducts which are high molecular weight complexes that might be less accessible to cells and may lower $[Ru(dip)_2(bpy\text{-}NitroIm)]^{2+}$ uptake (as discussed in the next paragraph). In the case of cisplatin, prolonging the time of incubation as well as addition of serum increased its cytotoxic effect. This suggests that distinct antiproliferative mechanisms are exerted by Ru compounds and cisplatin.

The influence of hypoxic conditions on the cytotoxicity of both Ru complexes as well as cisplatin was also evaluated. Ru compounds are found to be slightly more cytotoxic under hypoxic conditions. Hypoxic conditions usually results in a slower cell proliferation. Therefore, just based on IC_{50} parameter it difficult to conclude about the selectivity of hypoxia targeting drugs as was already shown for other compounds.[25] Therefore we have studied the influence of hypoxia on selected biological effects accompanying the treatment

Metallomics Accepted Manuscript

with Ru complexes to evaluate the possible hypoxia-selective properties of nitroimidazole derivative.

Antiproliferative activity of polypyridyl Ru complexes varies greatly. IC_{50} ranging from 0.7 μM ($[Ru(tpy)(Nh)_3]^{2+}$ (tpy is 2,2':6',2″-terpyridine, Nh is Norharman) on HeLa cell line[1] to more than 200 μM for Ru-coumarin derivatives (HepG2 cells)[2] that makes the studied compounds the most cytotoxic among the members of the of polypyridyl Ru complexes family.[3-10]

Cellular uptake of Ru complexes

The cytotoxicity of the studied Ru complexes might be directly related to their uptake by cells. The uptake of $[Ru(dip)_2(bpy\text{-}NitroIm)]^{2+}$ was monitored using flow cytometry and it was assumed that the light emitted by treated cells was proportional to the amount of Ru complex incorporated by cells. The studies performed in A549 and MLuMEC FVB cells (cancer and endothelial cells, respectively) showed that accumulation of the Ru complex inside the cells increased proportionally to the incubation time over the 24 h range (Fig. 1A and Figs. S1-S2). No saturation of uptake was observed up to 24 or 48 h for MLuMEC FVB and A549 cells, respectively, (Fig. 1A and Figs. S1-S2) suggesting a passive entry. It must be noted that the absence of serum resulted in an increase of the Ru complex uptake (Fig. S3) correlating with its higher cytotoxicity. Efficient uptake of the Ru complex is further confirmed by its accumulation in a dose-dependent manner (Fig. 1B).

Metallomics Accepted Manuscript

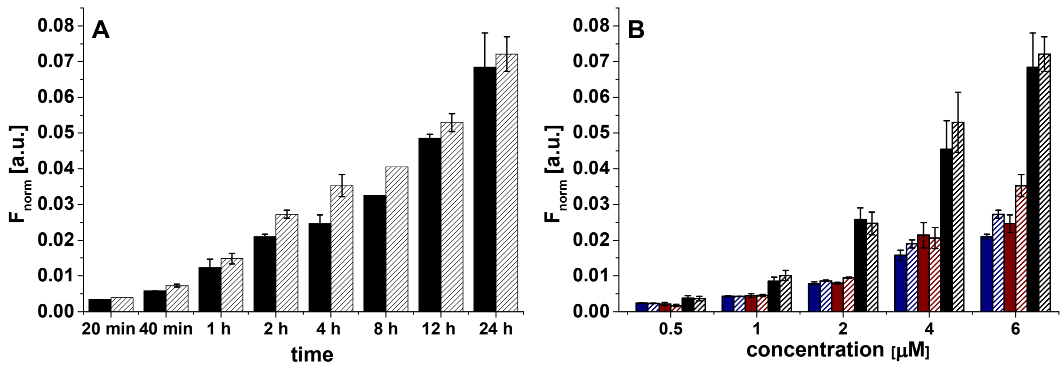

Fig. 1. Uptake of $[Ru(dip)_2(bpy\text{-}NitroIm)]^{2+}$ in MLuEC FVB cells conducted in the presence of 2% serum under normoxic (filled bar) and hypoxic (dashed bar) conditions. A) Time dependence ([Ru] = 6 μM) and B) concentration dependence after 2 (blue), 4 (red) and 24 h (black) incubation with cells.

The observed cellular concentration of the compound depends not only on the cellular uptake but also on the extent of efflux. Retention of $[Ru(dip)_2(bpy\text{-}NitroIm)]^{2+}$ was determined as the percentage of cell luminescence intensity left for additional 24 h incubation n Ru complex free medium as compared to the luminescence intensity measured immediately after 24 h of incubation with Ru complex. The outline of experiment is presented in Scheme S1. This further 24 h incubation allowed for the release of Ru complex from the cells. The amount of Ru complex remaining in cells represented 42 and 91% for MLuEC FVB and A549 cells, respectively. Such a relatively high efflux from the endothelial cells in comparison to cancer cells can indicate a beneficial effect in cancer treatment.

The presence of a nitroimidazole moiety in $[Ru(dip)_2(bpy\text{-}NitroIm)]^{2+}$ makes it to be expected that accumulation will be superior in hypoxia in cells expressing nitroreductase. Hypoxia induced nitroreductase was expressed only in MLuMEC FVB and A549 cells as detected using Cyto-ID Hypoxia/Oxidative stress detection kit. Accordingly, MLuMEC FVB cells exhibited higher accumulation of $[Ru(dip)_2(bpy\text{-}NitroIm)]^{2+}$ when kept in hypoxia for each incubation time (Fig. 1). Similar behavior exhibited A549 cells.[13] On the contrary, in

Metallomics Accepted Manuscript

4T1 cells only for short (≤ 2h) incubation time higher luminescence intensity was observed for cells cultivated under oxygen-deprived conditions while after 4 or 24 h the difference disappeared (Fig. S4). When accumulation study was carried out in medium without serum, the effect of hypoxia as inducer for higher accumulation of $[Ru(dip)_2(bpy\text{-}NitroIm)]^{2+}$ was even more pronounced in MLuMEC FVB (Fig. S5) and A549 [13] cells.

Mechanism of cellular uptake

MLuMEC FVB or A549 cells were used for further investigation regarding the underlying mechanisms of $[Ru(dip)_2(bpy\text{-}NitroIm)]^{2+}$uptake. To determine the role of nitroimidazole moiety in the uptake, some studies were also performed for $[Ru(dip)_2(bpy)]^{2+}$. Both complexes are transported into the cells rather than associating at the surface of the membrane. As shown in Fig. 2B or 3B $[Ru(dip)_2(bpy\text{-}NitroIm)]^{2+}$ stains homogeneously the cytoplasm with edge of the nucleus (mitochondria/endoplasmic reticulum) pointed out, suggesting that these organelles are the primary uptake place for the studied Ru compounds. To determine subcellular localization of Ru complex, organelle-specific dyes were used. After incubation of A549 cells with sub lethal dose of $[Ru(dip)_2(bpy\text{-}NitroIm)]^{2+}$ for 24 h it showed primary localization in mitochondria (Fig. 2) and endoplasmic reticulum (ER, Fig. 3) with excellent superimposition of organelle-specific dye with the studied Ru complex. The studies performed using confocal microscopy confirmed the accumulation of Ru complex in mitochondria while excluding the Golgi as a target (Fig. S6). Additionally the analysis of the luminescence intensity profiles revealed that $[Ru(dip)_2(bpy\text{-}NitroIm)]^{2+}$ was not localized in the nucleus (Fig. 2D and 3D). On the contrary, in the fixed cells the staining of nucleus was observed. Generally the fixed cells were stained more intense and quickly than alive cells

Metallomics Accepted Manuscript

(Fig. S7). This indicates that membrane permeability is one of the important factors of Ru complex uptake and the passive diffusion might be one of the ways to enter the cells.

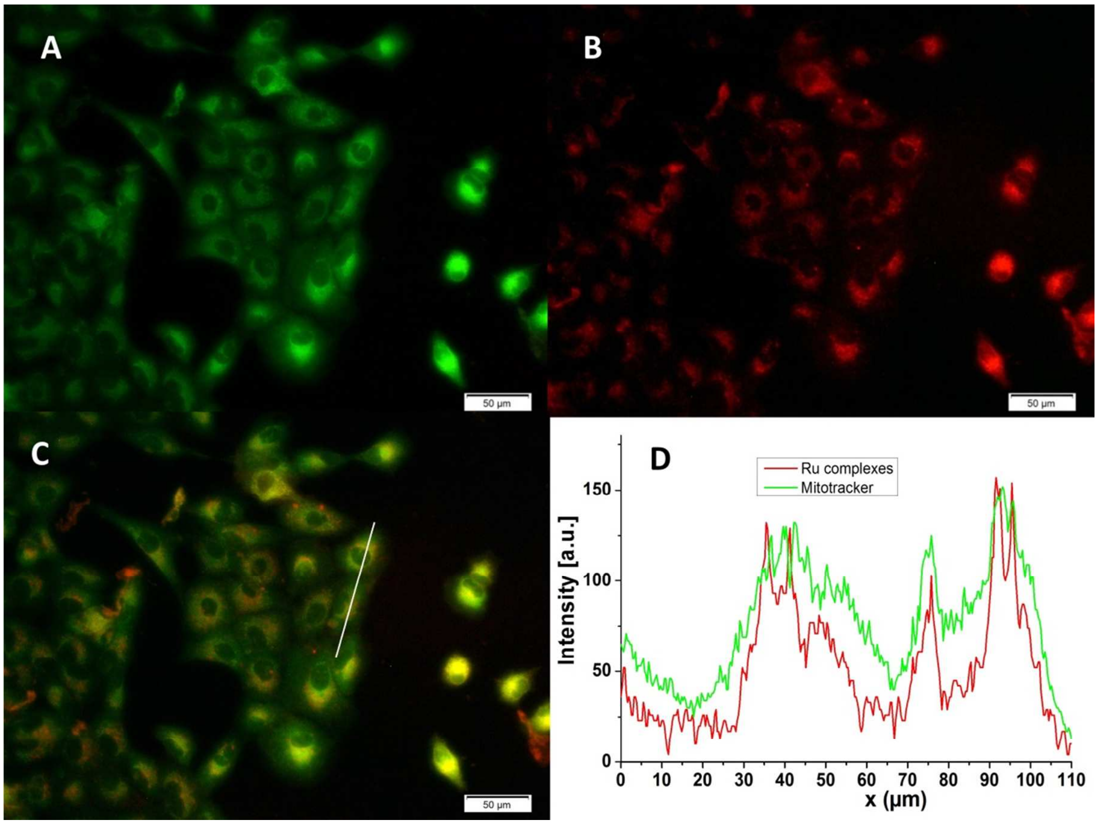

Fig. 2. Fluorescence images of A549 cells showing subcellular localization of $[Ru(dip)_2(bpy\text{-}NitroIm)]^{2+}$. (A, C) Mitotracker Green was used to image mitochondria and green color arises from organelle-specific dye; (B) red color denotes intrinsic emission of Ru complex (2 μM, 24 h of incubation at 37 °C). (C) The yellow color occurs due to the overlap of the red luminescence from the $[Ru(dip)_2(bpy\text{-}NitroIm)]^{2+}$ and green emission from dye, indicating co-localization. (D) Graph shows the luminescence intensity of both fluorophore and complex at boxed region. Scale bar is 50 μm.

Metallomics Accepted Manuscript

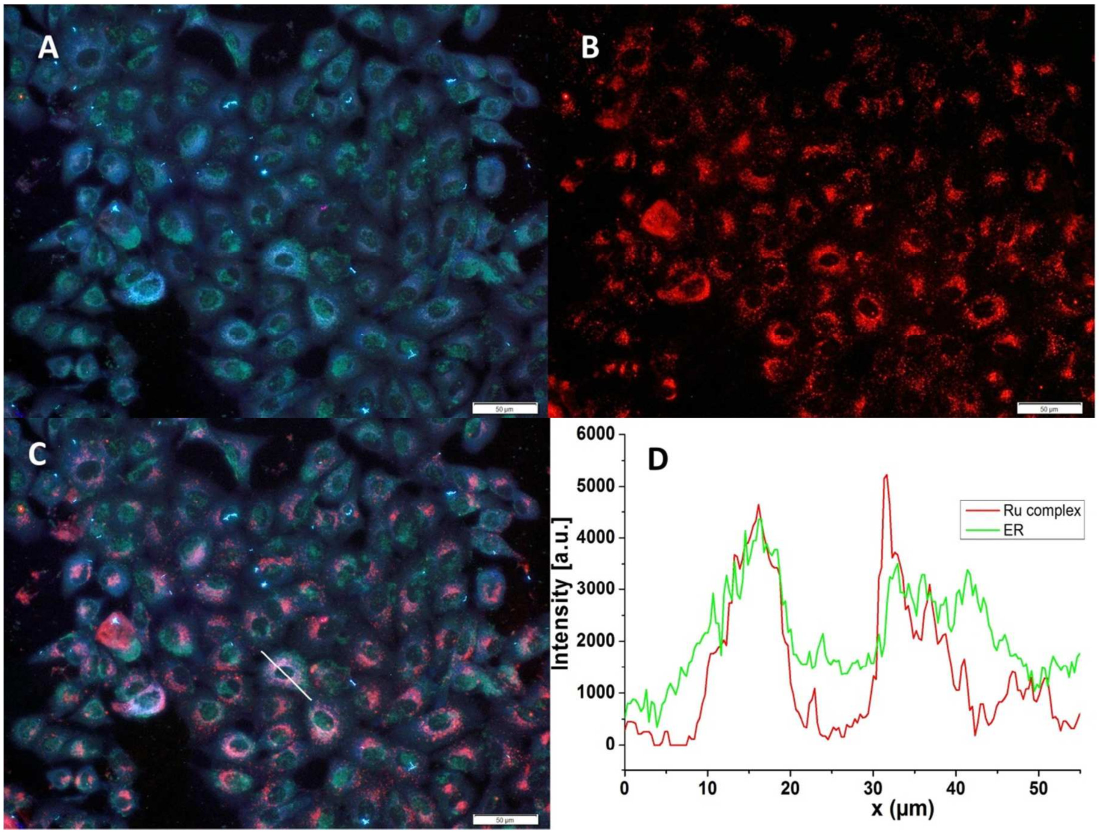

Fig. 3. Fluorescence images of A549 cells showing subcellular localization of $[Ru(dip)_2(bpy\text{-}NitroIm)]^{2+}$. (A, C) ER-Tracker™ Blue-White DPX was used to image endoplasmic reticulum and blue color arises from organelle-specific dye. (B) Red color denotes intrinsic emission of Ru complex (2 μM, 24 h of incubation at 37 °C). (C) The purpule-pink color occurs due to the overlap of the red luminescence from the $[Ru(dip)_2(bpy\text{-}NitroIm)]^{2+}$ and blue emission from dyes, indicating co-localization. (D) Graph shows the luminescence intensity of both fluorophores and complex at boxed region. Scale bar is 50 μm.

To determine whether the cellular uptake of the studied Ru compounds is energy-dependent, MLuMEC FVB cells were incubated with Ru complexes in the presence of various metabolic inhibitors. ATP depletion was conducted using glycolysis (deoxyglucose[26, 27] and iodoacetate[28]) and oxidative phosphorylation (azide[26]) inhibitors. The cellular uptake of

Metallomics Accepted Manuscript

$[Ru(dip)_2(bpy)]^{2+}$ remained essentially the same upon addition of metabolic inhibitors (Fig. 4A) indicating an energy-independent mechanism of uptake like passive or facilitated diffusion. In contrast, $[Ru(dip)_2(bpy\text{-}NitroIm)]^{2+}$ co-incubated with both deoxyglucose and azide showed a distinct change in its uptake profile (Fig. 4B), displaying a 50% decrease of the original value (from 38 ± 15 to 19 ± 7). Deoxyglucose alone caused only a moderate decrease in luminescence value (to 29 ± 11). These findings suggest that the transport of nitroimidazole-attached compound is partly energy-dependent, indicating a contribution of endocytosis or active transport proteins in the uptake of Ru complexes. It has been already proven that uptake of $[Ru(dip)_2(dppz)]^{2+}$ (where dppz is dipyridophenazine) is not dependent on cation transport inhibitors,[26] which might suggest a similar behavior of the present compounds.

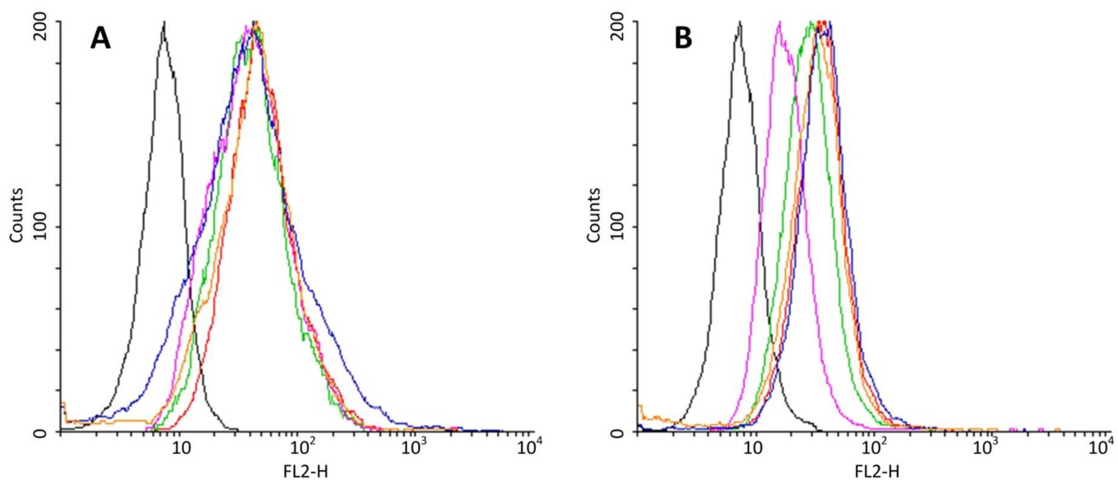

Fig. 4. Uptake of $[Ru(dip)_2(bpy)]^{2+}$ (A) and $[Ru(dip)_2(bpy\text{-}NitroIm)]^{2+}$ (B) by MLuMEC FVB cells after co-incubation with various metabolic inhibitors for 1 h, [Ru] = 2 μM (black – control, red – Ru, blue – Ru + iodoacetate (0.2 mM), orange – Ru + azide (3 mM), green – Ru + 2-deoxy-D-glucose (50 mM), pink – Ru + deoxyglucose (50 mM) + azide (3 mM)); λ_{ex} = 488 nm, λ_{em} = (575 ± 13) nm.

Metallomics Accepted Manuscript

A decrease of incubation temperature from 37 to 4 °C resulted in almost complete reduction of Ru complexes uptake (Fig. S8). It may suggest an energy-dependent transport but also may account for passive diffusion. The decreased membrane fluidity can alter diffusion of the Ru complexes.[29] Membrane cholesterol depletion was performed to determine how the membrane fluidity influences on Ru complexes uptake. Methyl-β-cyclodextril (MβCD) was used to extract cholesterol from cell membrane.[30, 31] MβCD forms soluble complexes with cholesterol depleting it from the cell membrane thus increasing membrane viscosity. After pre-incubation with MβCD the luminescence expressed by MLuMEC FVB cells treated with Ru complexes was reduced from 27 ± 10 to 10 ± 3 and from 16 ± 5 to 9 ± 3 for $[Ru(dip)_2(bpy)]^{2+}$ and $[Ru(dip)_2(bpy\text{-}NitroIm)]^{2+}$, respectively (Fig. S9). The lower uptake of both Ru complexes due to higher membrane rigidity suggests passive diffusion as a mechanism of entry. MβCD can also inhibit endocytosis [32, 33] and this mechanism is also suggested by the dot-like staining pattern of labelling (Fig. S10).

Plasma membrane of viable cells exhibits a membrane potential ranging from -50 to -70 mV, the inner part of the cell being negative as compared to the outer one.[26] Depolarization of the cell membrane generated by incubation with gramicidin (a hydrophobic linear polypeptide which forms channels in phospholipid membranes and allows ions to pass freely through the membrane, thus reducing its potential[29, 34]) reduced the uptake of both compounds (Fig. S11). Mean luminescence expressed by untreated/gramicidin-treated cells decreased from 138 ± 62 to 44 ±18 and from 34 ± 11 to 25 ±10 for $[Ru(dip)_2(bpy)]^{2+}$ and $[Ru(dip)_2(bpy\text{-}NitroIm)]^{2+}$, respectively. Whereas hyperpolarization of cell membrane created by addition of valinomycin (a cyclododecadepsi-peptide ionophore antibiotic, which allows the potassium ions passing freely through the cell membrane and in this way the interior voltage becomes more negative[35]) caused higher uptake of both Ru complexes. Co-incubating cells with valinomycin and Ru compounds resulted in an increase of the mean luminescence

Metallomics Accepted Manuscript

of cells from 27 ± 10 to 66 ± 28 and 21 ± 7 to 39 ± 18 for $[Ru(dip)_2(bpy)]^{2+}$ and $[Ru(dip)_2(bpy\text{-}NitroIm)]^{2+}$, respectively (Fig. S12). These studies have shown that uptake of the dicationic Ru complexes is facilitated by the potential difference across the cell membrane.

To assess whether the protein-mediated transport can be involved in the uptake of Ru complexes, the influence of Amphotericin B an antifungal drug, which can form pores in cell membrane, on Ru accumulation was investigated. Co-incubation with Amphotericin B did not influence the accumulation of the studied Ru compounds therefore it suggests that protein-mediated transport does not participate in their uptake.

Additionally, the role of copper transport protein CTR1 in cellular accumulation of Ru complexes was checked since it participates in the uptake of cisplatin. Co-incubation of MLuMEC FVB cells with various concentrations of $CuCl_2$ did not influence the accumulation of both Ru complexes. This observation excludes the CTR1 pathway as a possible route for the tested Ru polypyridyl complexes uptake.

Summarizing, $[Ru(dip)_2(bpy)]^{2+}$ enters cells by passive diffusion in a membrane-potential-related manner, similar as $[Ru(dip)_2(dppz)]^{2+}$.[26] Nitroimidazole-attached complex besides entering cells in an energy-independent way (passive diffusion facilitated by membrane potential) can be accumulated by an energy-depending pathway (probably endocytosis). Endocytosis was also suggested as transporting pathway for polypyridyl Ru conjugates with short peptides[36] as well as for bigger complexes for example highly-functionalized Ru(II) tris-bipyridine complexes[37] or binuclear Ru(II) polypyridyl complexes.[38]

Apoptosis-inducing and cell-cycle arresting properties of Ru complexes

Metallomics Accepted Manuscript

4T1 cells, upon incubation with the Ru compounds showed marked morphological sign of apoptosis, such as rounding and cell shrinkage.[24] Representative images are shown in Fig. S13. To evaluate the nucleus morphological changes, cells were stained with Hoechst 33258 and later analyzed by fluorescence microscopy. The untreated population of cells displays a homogenous morphology with nuclei evenly stained with Hoechst 33258. After treatment, most of the cells display fragmented nuclei with densely stained nucleus granular bodies of chromatin (so called “apoptotic bodies”).[10, 24, 39, 40]

The apoptosis-induced properties of Ru complexes were evaluated quantitatively using Annexin V/DAPI assay. The flipped phosphatidylserine of the cytoplasmic membrane at the early stage of apoptosis becomes available on the cell surface for binding with Annexin V. The percentage of living, necrotic and apoptotic A549 cells upon treatment with Ru complexes is shown in Fig. 5. The presence of $[Ru(dip)_2(bpy\text{-}NitroIm)]^{2+}$ and $[Ru(dip)_2(bpy)]^{2+}$ increased similarly the population of apoptotic cells while the necrotic cells represented only a minor fraction.

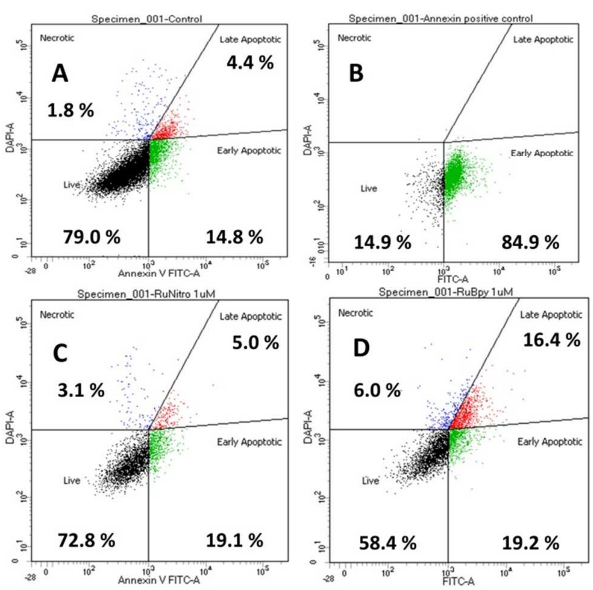

Metallomics Accepted Manuscript

Fig. 5. Apoptosis of A549 cells upon exposure for 24 h to (A) – control, (B) – H_2O_2 (6%), (C) $[Ru(dip)_2(bpy\text{-}NitroIm)]^{2+}$(1 μM) and (D) $[Ru(dip)_2(bpy)]^{2+}$ (1 μM), Cells were labeled with Annexin V-FITC/DAPI.

The influence of the Ru complexes on cell cycle progression was examined on 4T1 (Fig. 6) and MLuMEC cell lines by flow cytometry using staining with propidium iodide. Results showed that after a 24 h treatment, Ru complexes caused a reduction in G_0/G_1 phase accompanied by a corresponding increase in the percentage of cells in S phase. This data suggests that the antiproliferative mechanism of tested Ru polypyridyl complexes is based on S-phase arrest. Similar results were obtained for other Ru complexes.[6, 17]

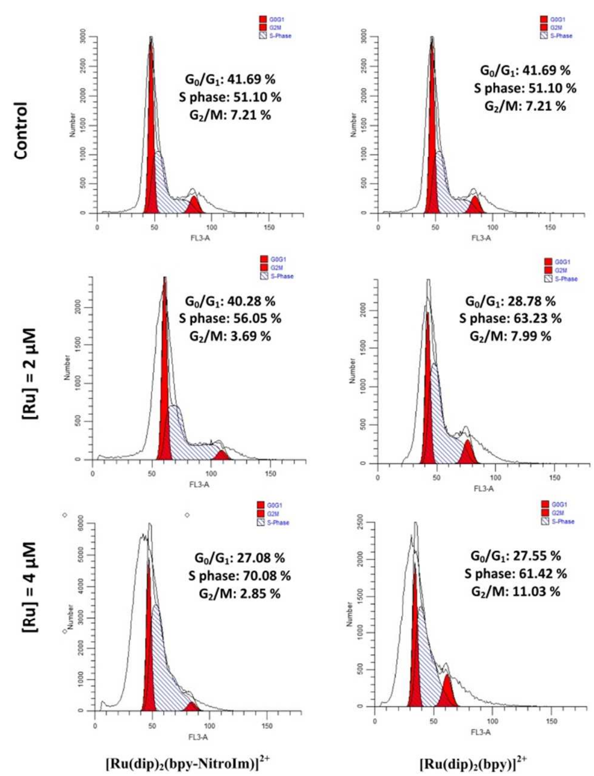

Fig. 6. Cell cycle distribution of 4T1 cells after 24 h treatment with Ru complexes.

Metallomics Accepted Manuscript

Many of the cell responses such as apoptosis or cell cycle arrest are known to be mediated by the production of reactive oxygen species. The level of oxidative stress induced by Ru complexes was evaluated and results are shown in Table 2. Ru complexes displayed a strong ability to induce oxidative stress in 4T1, A549 and MLuMEC FVB cell lines. $[Ru(dip)_2(bpy\text{-}NitroIm)]^{2+}$ showed a stronger oxidative stress inducing ability than $[Ru(dip)_2(bpy)]^{2+}$, despite its worse cell accumulation. This suggests an additional contribution of nitroimidazole moiety in the general oxidative stress effect. A549 and MLuMEC FVB cell lines were more sensitive toward Ru complexes than 4T1 cell line, which correlates with the expression of nitroreductase restricted to these two cell lines.

Table 2. The level of oxidative stress induced in 4T1, A549 and MLuMEC FVB cells after 24 h treatment with Ru complexes (2 μM) in normoxia expressed as percentage of cell population (%).

	4T1	A 549	MLuMEC FVB
Control	5 %	19 %	4 %
ROS Inducer (Pyocyanin)	65 %	73 %	89 %
$[Ru(dip)_2(bpy\text{-}NitroIm)]^{2+}$	35 %	95 %	93 %
$[Ru(dip)_2(bpy)]^{2+}$	15 %	94 %	79 %

Influence on cell adhesion

During the process of metastasis, tumor cells may leave the primary site, travel via blood or lymphatic systems, attach to a new distant site and establish a new secondary tumor.[41] These stages require essential mechanisms namely angiogenesis, degradation of the extracellular matrix, cell-cell and cell-matrix adhesion molecules and induction of cell motility.

Metallomics Accepted Manuscript

Both Ru complexes were tested for their influence on adhesion properties. As a model system to test cell detachment the resistance to trypsin had been measured. Diluted trypsin solution and short time of exposure were combined to avoid cell damage. As shown in Fig. S14 exposure of 4T1 cells to $[Ru(dip)_2(bpy\text{-}NitroIm)]^{2+}$ significantly increased cell adherence evaluated as the percentage of remaining adherent cells upon controlled trypsin treatment. Effect is more pronounced on collagen surface and seems to be not dependent on Ru complex concentration in the range from 0.75 to 3 μM. On plastic a pro-adhesive effect is less pronounced and increased with the Ru complex concentration. $[Ru(dip)_2(bpy)]^{2+}$ also enhanced 4T1 cancer cells adhesive properties, but a distinct effect was observed only for the lowest Ru complex concentration (0.75 μM). The same effect was observed upon collagen coating. MLuMEC endothelial cells adhesion properties were not significantly modified by Ru-nitroimidazole conjugate in terms of cell numbers resistant to trypsin treatment both on coated and uncoated surfaces. Low concentration of $[Ru(dip)_2(bpy)]^{2+}$ (0.75 μM) increased the numbers of adherent cells, while effect was reversed at higher concentrations. The observed differences between the studied cell lines one cancerous (4T1) and one non transformed (MLuMEC) suggest different molecular adhesion mechanism as evidenced by their response to treatment by Ru compounds. It is likely that such effect of Ru complexes on cancer cells, decreasing their detachment ability, might contribute to inhibition of cancer cell spreading.

On the contrary, in the secondary sites the pro-adhesion properties of cancer cells are crucial for attachment and proliferation. The influence of $[Ru(dip)_2(bpy\text{-}NitroIm)]^{2+}$ and $[Ru(dip)_2(bpy)]^{2+}$ on adhesion properties by assessing the ability of treated cells to attach to different types of coating was investigated for endothelial MLuMEC and cancer 4T1 cells. Treatments with both Ru complexes resulted in significant decrease of cell adhesion (Fig. 7). Changes of the cell adhesion properties on fibronectin, collagen and plastic were evidenced at

Metallomics Accepted Manuscript

incubation times as short as 4 h. Cell adhesion decrease was stronger for $[Ru(dip)_2(bpy)]^{2+}$. The Ru complexes inhibited attachment of both endothelial MLuMEC and cancer 4T1 cells which is favorable in view of anti-metastatic treatment.

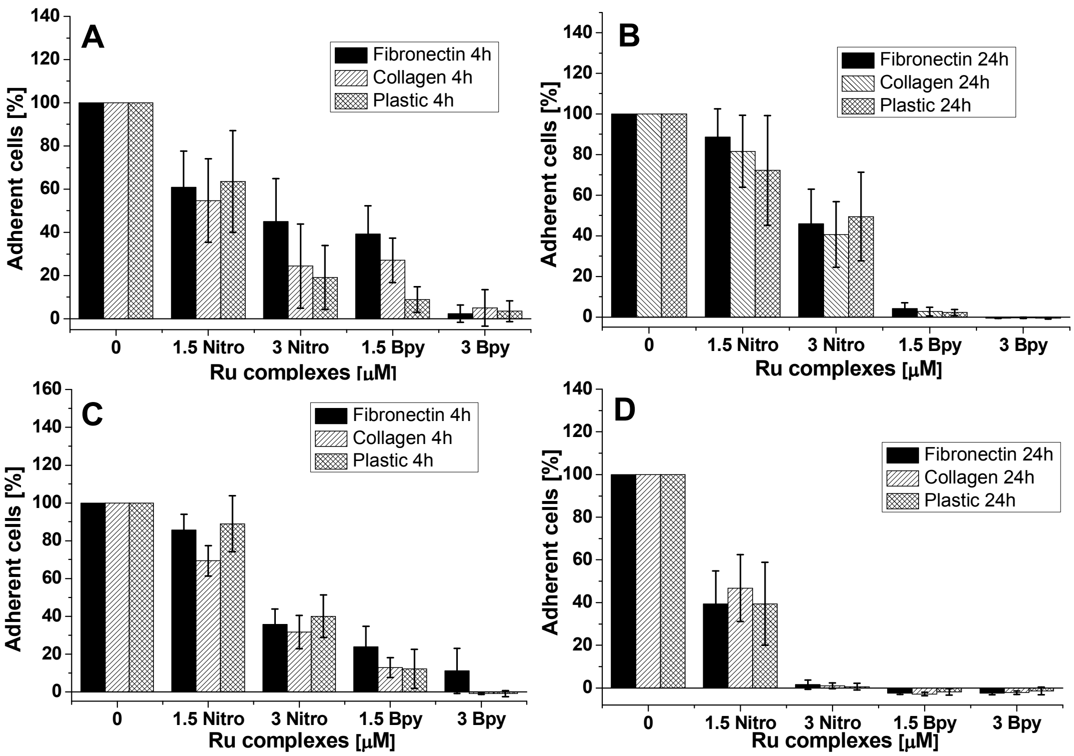

Fig. 7. Effect of $[Ru(dip)_2(bpy\text{-}NitroIm)]^{2+}$ (Nitro) and $[Ru(dip)_2(bpy)]^{2+}$ (Bpy) on MLuMEC endothelial cells (A, B) and 4T1 cancer cells (C, D) adhesion to fibronectin, collagen and plastic. Adhesion was measured after 4 h (A, C) and 24 h (B, D).

Since metastasis is the primary cause of mortality in cancer patients,[15] and breast cancer metastasize in lungs,[15] adhesion of Ru-treated 4T1 cells on lung endothelial MLuMEC FVB cells was also investigated (Fig. 8).[21] Incubation with the Ru complexes resulted in a dose-dependent reduction in 4T1 cells adhesion to MLuMEC FVB monolayer, noticeably 2 µM of $[Ru(dip)_2(bpy\text{-}NitroIm)]^{2+}$ underwent a drastic (98%) inhibition of 4T1 cell adhesion to MLuMEC FVB cells.

Metallomics Accepted Manuscript

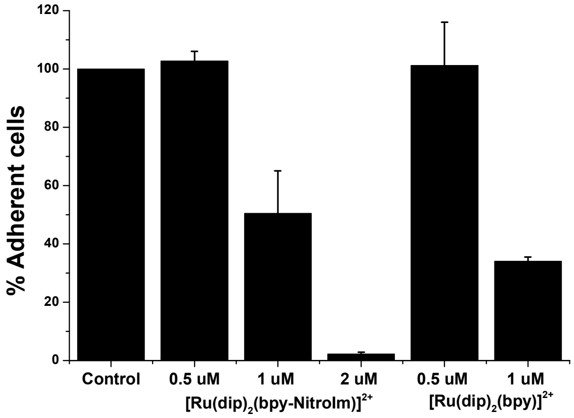

Fig. 8. Effect of $[Ru(dip)_2(bpy\text{-}NitroIm)]^{2+}$ and $[Ru(dip)_2(bpy)]^{2+}$ on 4T1 to MLuMEC FVB endothelial cells adhesion.

Effect on angiogenesis

The influence of Ru-nitroimidazole compound on the endothelial cells MLuMEC FVB angiogenesis was examined. It has been noticed that after several hours of incubation with the Ru complex MLuMEC FVB cells started to reorganize, showing tube-like and polygon structures. Tube formation was observed microscopically after 36 h of incubation in normoxia. Representative pictures are presented in Fig. 9 suggesting that the Ru complex can help in improving blood perfusion by re-arrangement of endothelial cells towards capillaries formation.

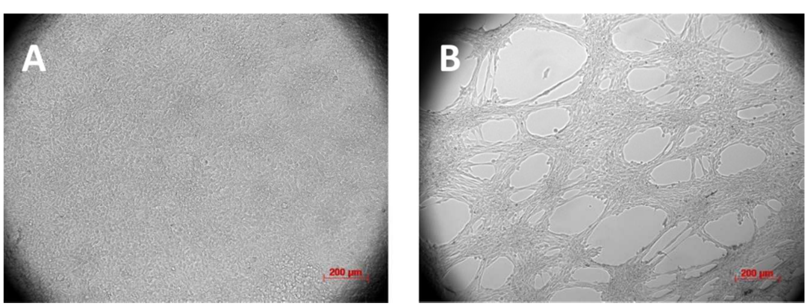

Metallomics Accepted Manuscript

Fig. 9. Effect of $[Ru(dip)_2(bpy\text{-}NitroIm)]^{2+}$ on angiogenesis of MLuMEC FVB cells. Pictures are taken after 36 h: (A) – control cells, (B) after incubation with 3 μM $[Ru(dip)_2(bpy\text{-}NitroIm)]^{2+}$, cells were seeded on plastic surface.

Such effect is particularly desired since it can inhibit the developing of hypoxia, while promoting normalization. It has been noted that classical anti-angiogenic treatments resulting in inhibition of new vessels formation can even increase hypoxia, thus select cancer stem like cells that are resistant to hypoxia and low pH. In turn, such cells are more aggressive and can lead to increase the invasiveness. .[18, 42, 43]

Moreover, effect of Ru complexes on cell mobility was assessed by wound healing assay. MLuMEC FVB cells monolayer was wounded, then incubated in fresh serum-free medium with various concentrations of $[Ru(dip)_2(bpy\text{-}NitroIm)]^{2+}$. Thymidine was added to arrest cell cycle allowing analyzing cell movement only and avoiding the cell division parameter. Control cells filled (77 ± 8)% of the scratched area after 11 h. The treatment of MLuMEC FVB cells with $[Ru(dip)_2(bpy\text{-}NitroIm)]^{2+}$ resulted in slight inhibition of their motility in a concentration dependent manner. After 11 h (68 ± 4) and (56 ± 6)% of scratched area were filled by cells upon incubation with 1 and 2 μM of Ru complex, respectively. The representative images are presented in Fig. 10.

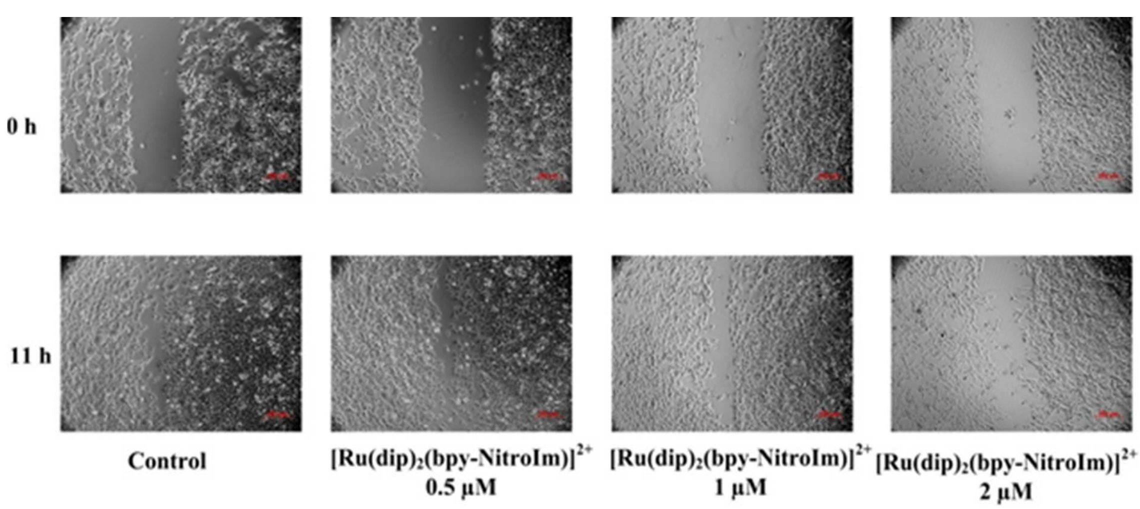

Metallomics Accepted Manuscript

Fig. 10. Representative images of wound healing assay: $[Ru(dip)_2(bpy\text{-}NitroIm)]^{2+}$ inhibition of MLuMEC FVB cells mobility.

Impact on the selected gene expression

The molecular mechanism underlying the biological effect of Ru complexes was assessed at the level of mRNA expression of several genes for both cancer (4T1) and endothelial (MLuMEC FVB) cells.

Tested Ru complexes had different impact on the expression level of the selected MMPs exhibited by 4T1 cells (Fig. 11). In normoxia, $[Ru(dip)_2(bpy\text{-}NitroIm)]^{2+}$ decreased the expression of MMP1a, MMP3, MMP9 in 4T1 cells. In hypoxia, a slight decrease of MMP1a expression (more pronounced by $[Ru(dip)_2(bpy)]^{2+}$) was observed. MMP9 expression only was significantly down regulated as opposed to MMP3 expression which was up regulated by $[Ru(dip)_2(bpy\text{-}NitroIm)]^{2+}$ treatment. The expression of TIMP1 (tissue inhibitor of metalloproteinases 1) underwent a slight increase, in hypoxia after $[Ru(dip)_2(bpy)]^{2+}$accumulation. In normoxia as well as hypoxia, both Ru complexes significantly down-regulated LOX (protein-lysine 6-oxidase). This protein is often up-regulated in hypoxic tumors, its expression promotes tumor growth and metastasis. THBS1 (thrombospondin-1) level was slightly decreased after incubation cells with Ru-nitroimidazole complex. This adhesive glycoprotein protein inhibits angiogenesis and plays a role in matrix stability and remodeling.[44] Reduction of its level suggests the demoting interaction between tumor cell and matrix. $[Ru(dip)_2(bpy)]^{2+}$ increased the level of integrin β 1, in normoxia, although it was significantly decreased in hypoxia. Since many integrins mediate tumor cell migration and invasion of the extracellular matrix,[45] decreased level of integrin β 1 after incubation with Ru complexes under hypoxic conditions can reduce cancer invasiveness.

Metallomics Accepted Manuscript

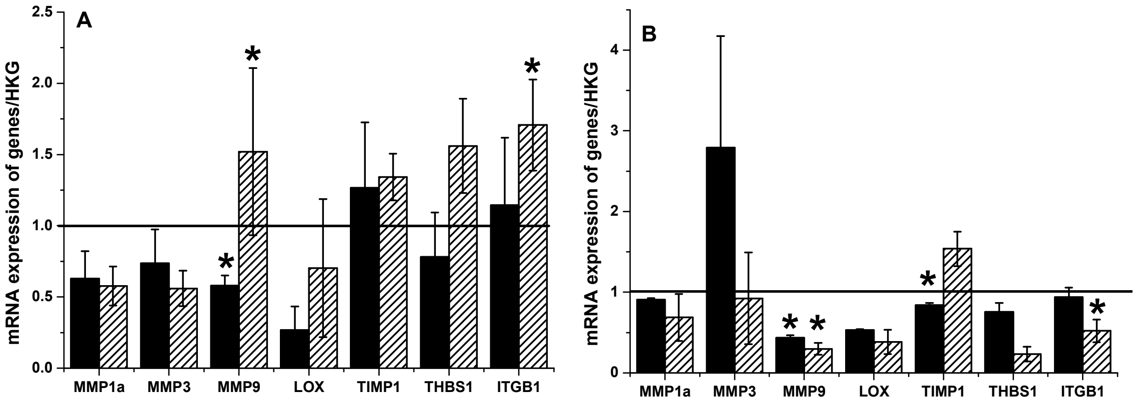

Fig. 11. Effect of Ru(dip)$_2$(bpy-NitroIm)]$^{2+}$ and [Ru(dip)$_2$(bpy)]$^{2+}$ on mRNA expression level of several matrix metalloproteinases (MMPs). The mRNAs were analyzed after 24 h incubation with [Ru(dip)$_2$(bpy-NitroIm)]$^{2+}$ (filled bars) and [Ru(dip)$_2$(bpy)]$^{2+}$ (dashed bars) under normoxic (A) and hypoxic (B,) conditions in 4T1 cell line. The results presented in graphs are means ± SEM of the experiments performed in three biological replicates. Student's t-test was used for statistical analyses: *$p<0.05$ was considered statistically significant.

The influence of both Ru complexes on the level of mRNA expression of genes for proteins important in cellular adhesion was also evaluated. Incubation of 4T1 cells with Ru complexes under normoxia revealed no change in CD44 expression while it increased under hypoxia. A similar effect was observed for CD34 expression; particularly, [Ru(dip)$_2$(bpy-NitroIm)]$^{2+}$caused a strong increase in the CD34 level in hypoxia (Fig. S15). This caused a slight increase in CD31 expression. CD146 (MCAM) level was differently modulated: while [Ru(dip)$_2$(bpy-NitroIm)]$^{2+}$ did not influence its expression, [Ru(dip)$_2$(bpy)]$^{2+}$, increased it in normoxia, whereas hypoxia diminished its expression level. In normoxia, Ru complexes increased the level of ICAM-1 (CD54), and VCAM-1 (CD106) while in hypoxia the effect of the Ru complexes was opposite. No significant influence was observed in the expression level of CD105 nor CD62E and Galectin3, but CD62P level decreased after treatment with Ru

Metallomics Accepted Manuscript

complexes under hypoxia (see Fig. S15). All these results show that both Ru complexes modify the level of gene expression of various adhesion molecules with different extent, suggesting anti-metastatic activity of Ru compounds. However more detailed studies comprising determination of the level of the expressed proteins are needed to confirm or decline this mode of action.

In endothelial cells MLuMEC FVB (Fig. S16) Ru complexes decreased the expression of LOX and MMP9 under hypoxic conditions, while causing no significant influence in normoxia. CD146 expression was strongly diminished by $[Ru(dip)_2(bpy)]^{2+}$ in hypoxia while $[Ru(dip)_2(bpy\text{-}NitroIm)]^{2+}$ increased it. CD31 expression underwent a drastic increase by Ru complexes (effect was stronger for $[Ru(dip)_2(bpy\text{-}NitroIm)]^{2+}$ - 6.4 times) under hypoxic conditions, whereas in normoxia mRNA expression remained unchanged. This is very important finding since it manifests a direct effect of the studied Ru complexes on vessel normalization. VCAM expression was significantly decreased in hypoxia by both Ru complexes. Although the $[Ru(dip)_2(bpy)]^{2+}$ diminished the expression of CD62E by 0.2 times, $[Ru(dip)_2(bpy\text{-}NitroIm)]^{2+}$, strongly increased (2.4 times) it in hypoxia. Galectin3 expression increased by $[Ru(dip)_2(bpy)]^{2+}$ (1.9 times) in hypoxia.

The hypoxia-regulated gene expression was followed in 4T1 and endothelial cells (summarized in Fig. S15 and Fig. S16). In 4T1 cells, HIF-1 gene (hypoxia induced factor 1) was slightly increased by $[Ru(dip)_2(bpy\text{-}NitroIm)]^{2+}$ in hypoxia only but the opposite effect was observed upon $[Ru(dip)_2(bpy)]^{2+}$ treatment. The expression of PHD2 (prolyl hydroxylase domain-containing protein 2) displayed the same tendency. PHD2 is the primary regulator of HIF-1α steady state level in the cell and some studies suggest that inhibition of the PHD2-HIF1 axis caused a decrease in tumorgenesis.[39] VEGFA (vascular endothelial growth factor A) gene expression was increased after incubation with Ru complexes under normoxic conditions, but decreased in hypoxia upon action of Ru compounds. It should be noted that a

Metallomics Accepted Manuscript

stronger effect was observed by $[Ru(dip)_2(bpy)]^{2+}$, possibly due to its better cellular uptake. VEGFR2, a receptor of VEGF protein was modulated similarly. VEGF promotes angiogenesis and cell migration. Many drugs like bevacizumab and ranibizumab monoclonal antibodies which can reduce the quantities of VEGF are approved for anticancer treatments.[46-48] mRNA profile of MLuMEC cells after treatment with Ru complexes was significantly different from the results obtained for 4T1 cell line (Fig. S15 and Fig. S16). No influence on the expression of HIF1 was observed, while PHD2 expression was significantly lower after incubation with Ru complexes under hypoxic conditions and slightly higher after incubation under normoxic conditions. VEGF expression was increased after treatment with Ru complexes under normoxic conditions, while under hypoxic conditions expression of this mRNA was considerably lower. On the contrary VEGFR2 expression was not changed, and only incubation with $[Ru(dip)_2(bpy)]^{2+}$ under hypoxia, boosted its expression.

Ru complexes differently impacted the expression of angiopoietins, key molecules for angiogenesis, in MLuMEC cells: whereas $[Ru(dip)_2(bpy\text{-}NitroIm)]^{2+}$ had no significant influence, incubation with $[Ru(dip)_2(bpy)]^{2+}$ strongly increased the expression of ANGPT2, while the level of ANGPT1 was diminished. CD202B is the receptor for angiopoietins; its expression was increased after incubation under normoxia, the effect was stronger by $[Ru(dip)_2(bpy)]^{2+}$ treatment (Fig. S16) while in hypoxia the influence of Ru complexes was marginal.

CONCLUSIONS

The present study introduces an additional aspect of anticancer activity of Ru polypyridyl complexes. The investigated Ru complexes possess higher cytotoxic potency than widely used clinical chemotherapeutic agent cisplatin. Their antiproliferative activities may be

Metallomics Accepted Manuscript

caused by cell cycle arrest at the S-phase. Further studies show that complexes can induce apoptosis through ROS generation.

Tested Ru complexes can not only act as cytotoxic agents but they very likely, possess anti-metastatic activity. Ru complexes change the adhesion properties of the treated cells. They decrease the amount of adherent cells to different surface (fibronectin, collagen, plastic) both for endothelial MLuMEC and cancer 4T1 cell lines. Additionally, after incubation with Ru complexes the resistance of 4T1 cells to trypsin treatment increases. Ru complexes successfully inhibit adhesion of treated 4T1 cells on the endothelial MLuMEC cells. In addition, they decrease the expression of several matrix metalloproteinases as well as protein-lysine 6-oxidase and increase the expression of extracellular matrix inhibitor, which play important role in spreading of cancer cells. Moreover, it was shown that their retention in endothelial cells is much lower than in cancer 4T1 cells. Faster clearance of Ru complexes from endothelial cells can account for lower host toxicity. Although Ru complexes are also cytotoxic against endothelial cells, which might cause undesired effects, their influence on formation tube-like and polygon structures appears beneficial. Indeed, it seems from these preliminary data that Ru complexes have a strong influence on the molecules that govern the state of the endothelial cells and that they increase the molecules that maintain the normal vessel function. This is a potentially important feature that makes the Ru derivatives interesting for angiogenesis based treatments. This process is mainly visible in hypoxia which relates directly to tumor real conditions. All these findings are relevant towards inhibition of metastasis. In our opinion the future work should concentrate on confirming this property by *in vivo* study.

EXPERIMENTAL SECTION

Studied metal complexes

Metallomics Accepted Manuscript

$[Ru(dip)_2(bpy\text{-}2\text{-}nitroIm)]Cl_2$ and $[Ru(dip)_2(bpy)]Cl_2$ were prepared according to published procedures.[13] Ru compounds were freshly dissolved in DMSO and then added to the appropriate medium. Final DMSO concentration was kept constant at 0.05 % (v/v) in all experiments, except cytotoxic study using A549 cell line (0.2%). Cisplatin was purchased from Sigma-Aldrich and diluted in water/medium prior the experiments.

Cell lines and cell culture

FVB mouse lung microvascular endothelial cells (MLuMEC FVB) and murine endothelial cells isolated from aorta-gonad-mesonephros (AGM) region of 10.5 dpc embryos (MAgEC 10.5) were cultured in OptiMEM with Glutamax-I (Gibco Invitrogen) supplemented with 2% fetal bovine serum (FBS), 0.4% gentamycin and 0.2% fungizone. 4T1 breast cancer cell line was cultured in RPMI-1640 (Gibco Invitrogen) with 10% FBS, 1% peniciline and streptomycin and 0.2% fungizone. Human lung adenocarcinoma epithelial cell line (A549) was cultured in DMEM (Gibco Invitrogen) with 10% FBS, 1% peniciline and streptomycin and 0.2% fungizone. Cells were routinely cultured at 37 °C in a humidified incubator in 5% CO_2 atmosphere. For hypoxia treatments, cells were placed in a humidified atmosphere containing 1% of oxygen in a hypoxic station Whitley H35. This oxygen pressure was obtained by introducing 94% N_2, 5% CO_2 and 1% O_2 gas mixture. Cells intended for hypoxic experiments were preincubated at hypoxic chamber for at least 12 h.

Cytotoxicity assay

Cell viability was measured using Alamar Blue assay. Cells were seeded on 96 wells plate with density of 1×10^4 cells per cm^2 and cultured for 1 day. Then cells were incubated with various concentrations of compounds in medium with or without 2% FBS for 24 and 48 h under normoxic and hypoxic conditions in the darkness. Next cells were washed with PBS

Metallomics Accepted Manuscript

and incubated in Alamar Blue solution for 3 h. The cell viability was quantified at 605 nm using 560 nm excitation light (VICTOR 3V multilabel plate reader PerkinElmer or Tecan Infinite200 Reader). Experiments were performed in triplicates and each experiment was performed at least three times to get the mean values ± standard derivation. The viability was calculated with regard to the untreated cells control. The IC_{50} values were determined using Hill equation (Origin 9.0) [49].

$$y = y_0 + \frac{(y_{100} - y_0)[c]^H}{[IC_{50}]^H + [c]^H}$$

General remarks to flow cytometry experiments

For all described below experiments a special care was undertaken to asses only the live cells. It was achieved by applying sub-lethal dose of Ru complex and analyzing only sub-population of singular events in flow cytometry measurements. The chosen dosage of Ru compounds depends on *i*) cellular density, *ii*) time of incubation and *iii*) the presence of serum in incubation medium and was individually selected for each experiment. The cellular uptake of $[Ru(dip)_2(bpy\text{-}NitroIm)]^{2+}$ and $[Ru(dip)_2(bpy)]^{2+}$ was monitored by following the luminescent signal of treated cells using flow cytometry. Cells were analyzed by BD LSR, BD FacsSORT or BD LSRFortessa cytometers equipped with FACSDiva (BD Biosciences) software. Also Flowing Software was partially used to analyze data. Experiments were performed under normoxic conditions until stated otherwise.

Time and concentration dependence uptake

To study time and concentration dependence uptake of $[Ru(dip)_2(bpy\text{-}NitroIm)]^{2+}$, A549 cells were seeded on a 6 wells plate with a density of 5×10^4 cells per cm^2 24 h prior the treatments. Cells were next incubated with various concentrations of the Ru complex (1 – 4 µM) for various periods of time (1 – 48 h). After the incubation cells were washed twice

Metallomics Accepted Manuscript

with PBS detached by trypsin treatment and analyzed by flow cytometer. MLuMEC FVB cells were seeded on 6 wells plates with a density of 1.6 × 10^4 cells per cm^2 24 h prior the experiments. Next $[Ru(dip)_2(bpy\text{-}NitroIm)]^{2+}$ was added at the various concentration (0 – 6 μM) and cells were incubated in medium with serum for different period of time. After the incubation cells were washed and later analyzed using flow cytometry.

Extent of efflux

MLuMEC FVB cells were seeded on 24 wells plates with a density of 2 × 10^4 cells per cm^2 cells per well 24 h prior the experiments. Next $[Ru(dip)_2(bpy\text{-}NitroIm)]^{2+}$ was added at the various concentration (0.5, 1, 2 μM) and cells were incubated in serum-free medium for another 24 h. After the incubation Ru complex was removed, cells were washed twice with PBS, trypsinisized and the first half of cells was analyzed by flow cytometry. Another half was seeded on the new well, fresh complete medium was applied, and cells were incubated again for another 24 h, treated with trypsin and analyzed by flow cytometry.

Cellular imaging of accumulated Ru complexes

MLuMEC FVB cells were seeded on round dishes (Ø 35 mm) with the density of 25 × 10^4 cells per dish 24 h prior the staining. In some of the dishes cells were fixed by addition of cold methanol at -20 °C for 15 min. After fixation cells were rinsed with PBS twice. Alive and fixed cells were stained with 6 μM $[Ru(dip)_2(bpy\text{-}NitroIm)]^{2+}$ in serum-free medium for 1 h at 37 °C. After incubation cells were washed with PBS and images were acquired using an AxioVert 200M fluorescence microscope (Carl Zeiss).

For co-localization experiments, A549 cells were seeded on a glass surface with a density of 10^4 cells per cm^2 24 h prior the staining. CellLight® ER-RFP, ER-Tracker™ Blue-White DPX, CellLight® Golgi-RFP (Molecular Probes, Life Technologies) and Mitotracker

Metallomics Accepted Manuscript

Green (Life Technologies) were used to image ER, mitochondria and Golgi according to manifacture's protocols. For colocalization with Mitotracker and ER-Tracker™ Blue-White DPX cells were incubated with 2 μM $[Ru(dip)_2(bpy\text{-}NitroIm)]^{2+}$ in complete medium for 24 h, then rinse twice with PBS. Images were acquired using Olympus fluorescence microscope IX51 equipped with XC10 camera with 470–495 and 530–550 nm excitation filters. Alternatively, to optimized the signal intensity in confocal microscopy, cells were incubated with 8 μM $[Ru(dip)_2(bpy\text{-}NitroIm)]^{2+}$ in complete medium for 40 min (ER and Golgi dyes), then rinse twice with PBS. Images were acquired using Nikon Ti-E microscope with 488 nm and 561 nm excitation wavelengths.

Mechanism of cellular uptake

MLuMEC FVB cells were used to explore mechanisms involved in $[Ru(dip)_2(bpy\text{-}NitroIm)]^{2+}$ and $[Ru(dip)_2(bpy)]^{2+}$ accumulation. Cells were seeded on 6 wells plates with a density of 1.6×10^4 cells per cm^2 24 h prior the experiments. For each experiment incubation was followed by detachment with trypsin, washing and analysing by BD LSR cytometer. To study if the mechanism of uptake of the Ru compounds is energy dependent MLuMEC FVB cells were depleted of their ATP stores using different metabolic inhibitors. Cells were pre-treated either with 50 mM 2-deoxy-D-glucose, 3 mM sodium azide, 0.2 mM iodoacetate or with a mixture of deoxyglucose and azide. After 1 h of pretreatment the Ru compounds (2 μM) were added and incubation continued for another hour at 37 °C. For evaluation of temperature influence on the Ru compounds uptake MLuMEC FVB cells were incubated at 37, 20 and 4 °C for 1 h with 2 μM Ru compounds. Effect of membrane fluidity was studied by using methyl-β-cyclodextrin (MβCD), which make membrane more rigid. MLuMEC FVB cells were pre-incubated with 10 mg/ml of MβCD for 30 min at 37 °C and followed by co-incubation for 1 h with 2 μM Ru complexes. To study if the changes in membrane potential

Metallomics Accepted Manuscript

influence on the Ru uptake co-incubations with gramicidin and valinomycin were performed. MLuMEC FVB cells were pre-incubated for 30 min at 37 °C with 50 μM valinomycin or 5 μM gramicidin. Next the Ru compounds at 2 μM concentration were added and incubation continued for another hour. To assess if copper transported protein CTR1 pathway is involved in Ru complexes accumulation MLuMEC FVB cells were incubated with 2 μM the Ru complexes for 24 h in the presence of 10, 20, 40 and 100 μM of $CuCl_2$. As a model of protein mediated transport co-incubation experiments with amphotericin B was used. MLuMEC FVB cells were incubated with 2 μM the Ru complexes for 24 h together with 1, 5, 10 and 20 μM of amphotericin B (basal level of amphotericin B presented in medium used for cell culture is 0.5 μM).

Accumulation under hypoxic conditions and ROS detection

Cellular uptake under hypoxic conditions was studied using MLuMEC FVB and 4T1 cell lines. MLuMEC FVB and 4T1 cells were seeded in a 24 wells plate with a density of 2×10^4 cells per cm^2. 24 h after the seeding Ru(II) compounds were added and incubated for different time period under normoxic and hypoxic conditions. Then cells were washed with PBS, treated with trypsin and analyzed by BD LSR cytometer. Additionally the cyto-ID Hypoxia/Oxidative stress detection kit was used to check if MLuMEC FVB, 4T1 and A549 cells express nitroreductase under both normoxic and hypoxic conditions. This kit also included the second reagent which allowed for simultaneously detection of the total reactive oxygen species (ROS) produced in the cell upon addition of Ru complex. As a positive control pyocyanin was used. The level of oxidative stress was determined in 4T1, A549 and MLuMEC FVB cells.

Apoptosis assay by Hoechst 33258 staining method

Metallomics Accepted Manuscript

4T1 cells were seeded into 96 wells plate with a density of 2 × 10^4 cells per cm^2 and cultured in the full medium for 1 day. The medium was removed then and replaced with medium containing different concentrations of the $[Ru(dip)_2(bpy\text{-}NitroIm)]^{2+}$. Cells were incubated with compound for 24 and 48 h, then washed with iced-cold PBS, fixed with formalin (4%). Cell nuclei were counterstained with Hoechst 33258 (10 µg/ml in PBS) for 15 min. Cells were then observed and imaged by fluorescence microscope AxioVert 200M fluorescence microscope (Carl Zeiss).

Apoptosis assay by flow cytometry

A549 cells were seeded into 6 wells plate with a density of 2 × 10^4 cells per cm^2 and cultured in the full medium for 1 day. Afterwards the medium was removed and replaced by medium containing 1 µM of $[Ru(dip)_2(bpy\text{-}NitroIm)]^{2+}$ and $[Ru(dip)_2(bpy)]^{2+}$ and incubated for 24 h. Then cells were washed with PBS and binding buffer (25 mM Hepes/NaOH pH 7.4, 140 mM NaCl, 5 mM KCl, 1 mM $MgCl_2$, 2.5 mM $CaCl_2$).The cells were stained with annexin V-FITC for 10 min in the dark and then with DAPI (0.5 µM) for 5 min. Cells were analyzed by BD LSRFortessa cytometer. H_2O_2 (6%) were used as positive controls.

Cell cycle arrest assay

4T1 cells were seeded into 6 wells plate with a density of 3 × 10^4 cells per cm^2 while MLuMEC FVB cells with a density of 2 × 10^4 cells per cm^2. Cells were cultured in the full medium for 1 day. Than the medium was removed and replaced with basic medium containing different concentrations of the $[Ru(dip)_2(bpy\text{-}NitroIm)]^{2+}$ and $[Ru(dip)_2(bpy)]^{2+}$ and were incubated for 24 h. Then cells were washed with PBS, detached by trypsin, fixed in cold methanol for 30 min, stained with propidium iodide (PI) for 4 h in the dark followed by analyzing using BD FacsSORT cytometer (λ_{ex} = 488 nm and λ_{em} = 585 ± 21 nm).

Metallomics Accepted Manuscript

Resistance to trypsin treatment

To evaluate the change in cells adhesion the resistance to trypsin treatment test was performed by a reported method[50] with a few modifications. Cells were seeded on uncoated bottom of plastic plate or on collagen coated surface on a 96 wells plate with a density of 1.5 × 10^4 cells per cm^2 (MLuMEC FVB) and 1.9 × 10^4 cells per cm^2 (4T1). 24 h after seeding the Ru complexes were added to the wells at different concentration ($[Ru(dip)_2(bpy\text{-}NitroIm)]^{2+}$: 0.75, 1.5 and 3 μM; $[Ru(dip)^2(bpy)]^{2+}$: 0.75, 1.5 and 2 μM). Wells with compounds were incubated in a humidified atmosphere at 37 °C for 24 h, then washed with PBS. Next trypsin solution (0.05% for 4T1 cells, 0.005 % for MLuMEC FVB cells) was added to each well and plates were incubated at 37 °C for 10 min (4T1 cells) or 5 min (MLuMEC FVB cells). Then cells were washed and Alamar Blue test was performed to quantify adherent cells. Experiments were performed in triplicates and each was repeated 5 times to calculate the mean values ± standard derivation. To eliminate possible toxicity of the compounds obtained results were normalized with the corresponded wells without trypsin treatment and presented as percentage of control wells.

Cell adhesion assay

Cell adhesion assay was performed by a reported method[50, 51] with a slight modification. Test was performed on various substrates: plastic (uncoated bottom of the plates), fibronectin from human plasma and collagen I from calf skin (Sigma). Briefly, fibronectin and collagen were diluted to 25 μg/ml with sterile water and wells of 96 well plate were coated at 4 °C overnight with 50 μl solutions. The wells were then washed 2 times with PBS. MLuMEC FVB and 4T1 cells were seeded with a density of 2 × 10^4 cells per cm^2 into 6 wells plate. 24 h after seeding Ru complexes were added to the wells at various

Metallomics Accepted Manuscript

concentrations (1.5 and 3 μM). Wells with compounds were incubated in a humidified atmosphere at 37 °C for 4 and 24 h. Next plates were washed with PBS, cells were detached with cell dissociation solution, counted and add to wells of 96 well plates with a density of 6 × 10^4 cells per cm^2. Plates were incubated in a humidified atmosphere at 37 °C for 1 h, then plates were washed to detached non adherent cells and Alamar Blue test was performed to quantify adherent cells. Experiments were performed in triplicates and each was repeated 5 times to calculate the mean values ± standard derivation. Results are presented as a percentage of control cells.

Adhesion of 4T1 cells on endothelial cells

MLuMEC FVB were seeded in a 24 well plate with a density of 2 × 10^4 cells per cm^2 2 days prior the experiments to achieve the monolayer. 4T1 cells were seeded with a density of 3 × 10^4 cells per cm^2 into 6 well plates and after 24 h of cultivation, the Ru complexes $[Ru(dip)_2(bpy\text{-}NitroIm)]^{2+}$ and $[Ru(dip)_2(bpy)]^{2+}$ were added at the various concentrations: 0.5, 1 and 2 μM. After 24 h of incubation 4T1 cells were detached, labeled with DiI (Life Technologies) according to manufacture instruction and counted. Labeled cells were added to a monolayer of MLuMEC FVB cells at the concentration ratio 4T1: MLuMEC FVB = 1:1. Cells were incubated for 1 h in serum free medium and then gently washed with PBS twice (to detach non adherent cells). Next cells were detached by trypsine and analyzed by flow cytometry. The experiment was performed in triplicate and repeated 3 times.

Migration assay (wound healing assay)

The wound healing assay was done to gain information about influence of the Ru complexes on the migration of MLuMEC FVB cells. Cells were seeded with a density of 0.8 × 10^4 cells per cm^2 two days before the experiments. A 20 μl pipette tip was used to scratch

Metallomics Accepted Manuscript

and create a wound in the monolayer of MLuMEC FVB cells. After washing with serum-free medium, the Ru complexes dissolved in serum free medium were added. The images showing migration of the cells into the cleared spaces were taken every hour for 72 h by an AxioVert 200M fluorescence microscope (Carl Zeiss). For analysis the scratches with the similar distance were taken and the presented results were calculated based on 4 independent experiments done in quadruplets.

Angiogenesis

MLuMEC FVB were seeded in a 96 well plate with a density of 3×10^4 cells per cm^2 10 h prior the experiments. Next $[Ru(dip)_2(bpy\text{-}NitroIm)]^{2+}$ was added at various concentrations (0 – 3 μM). The images were taken after 36 hours after the beginning of incubation.

Quantitative reverse transcription – polymerase chain reaction

Cells (4T1 and MLuMEC FVB) were seeded on a 35 mm dishes with a density of 10^6 cells per dish. 24 h after the seeding, 2 μM Ru complexes were added and cells were incubated for another 24 h under hypoxic and normoxic conditions. Next cells were washed and total RNA was harvested using RNeasy Plus Mini kit (Qiagen). Reverse transcription was performed using Maxima First Strand cDNA Synthesis Kit for RT-qPCR (Fermentas), and PCR was done with a SYBR Premix Ex Taq (Takara Bio Inc). The primers were used from QuantiTect Primer Assays (Qiagen). Experiments were performed in three biological replicates, for several genes (CD146, MMP1a, MMP9, VCAM, ICAM-1, LOX) repeated twice. PCR conditions were as follows: 30 s at 95 °C, and 55 cycles of 5 s at 95 °C, 20 s at 60 °C and 15 s at 72 °C. Fluorescence was measured on a LightCycler480 (Roche) thermal

Metallomics Accepted Manuscript

cycler. Data were analyzed according to the $2_T^{-\Delta\Delta C}$ method[52] and normalized by PPIA or GAPDH mRNA expression (housekeeping genes HKG) in each sample.

Statistical analysis of mRNA expression

Values are expressed as mean ± SEM. The statistical significance of differences between experiment and control groups was determined by Student's t-test with *p* values considered significant $*p < 0.05$. All statistical analyses were performed using Statistica v.10.

ACKNOWLEDGMENTS

Financial support from the National Science Center (grant no. N N204 247340) is acknowledged. The research was carried out with equipment purchased with financial support from the European Regional Development Fund within the framework of the Polish Innovation Economy Operational Program (contract no. POIG.0 2.01.00-12-0 23/08). O.M. acknowledges the financial support from the project Interdisciplinary PhD Studies "Molecular sciences for medicine" (co-financed by the European Social Fund within the Human Capital Operational Programme).

References

1. Y. Chen, M.-Y. Qin, L. Wang, H. Chao, L.-N. Ji, A.-L. Xu, *Biochimie,* 2013, **95**, 2050-2059.
2. M. J. Li, K. M. C. Wong, C. Yi, V. W. W. Yam, *Chem. Eur. J.,* 2012, **18**, 8727-8730.
3. H. J. Yu, Y. Chen, L. Yu, Z. F. Hao, L. H. Zhou, *Eur. J. Med. Chem.,* 2012, **55**, 146-154.
4. M. R. Gill, H. Derrat, C. G. W. Smythe, G. Battaglia, J. A. Thomas, *ChemBioChem,* 2011, **12**, 877-880.
5. C. Wang, Q. Yu, L. Yang, Y. Liu, D. Sun, Y. Huang, Y. Zhou, Q. Zhang, J. Liu, *Biometals,* 2013, **26**, 387-402.

Metallomics Accepted Manuscript

6. Q.-F. Guo, S.-H. Liu, Q.-H. Liu, H.-H. Xu, J. H. Zhao, H. F. Wu, X. Y. Li, J. W. Wang, *DNA Cell Biol.,* 2012, **31**, 1205-13.

7. K. K. W. Lo, T. K. M. Lee, J. S. Y. Lau, W. L. Poon, S. H. Cheng, *Inorg. Chem.,* 2008, **47**, 200-208.

8. A. Srishailam, Y. R. Kumar, N. M. D. Gabra, P. V. Reddy, N. Deepika, N. Veerababu, S. Satyanarayanna, *J. Fluoresc.,* 2013, **23**, 897-908.

9. J. X. Zhang, J. W. Zhou, C. F. Chan, D. W. J. Kwong, H. L. Tam, N. K. Mak, K. L. Wong, W. K. Wong, *BioConjugate Chem.,* 2012, **23**, 1623-1638.

10. Y.-Y. Xie, H.-L. Huang, J.-H. Yao, G.-J. Lin, G.-B. Jiang, Y.-J. Liu, *Eur. J. Med. Chem.,* 2013, **63**, 603-610.

11. A. C. Komor, J. K. Barton, *Chem. Commun.,* 2013, **49**, 3617-3630.

12. A. C. Komor, C. J. Schneider, A. G. Weidmann, J. K. Barton, *J. Am. Chem. Soc.,* 2012, **134**, 19223-19233.

13. O. Mazuryk, M. Maciuszek, G. Stochel, F. Suzenet, M. Brindell, *J. Inorg. Biochem.,* 2014, **134**, 83-91.

14. S. Kizaka-Kondoh, H. Konse-Nagasawa, *Cancer Sci.,* 2009, **100**, 1366-1373.

15. K. Ito, S. J. Ralph, *Clin. Exp. Metastasis,* 2012, **29**, 561-572.

16. S. Goel, D. G. Duda, L. Xu, L. L. Munn, Y. Boucher, D. Fukumura, R. K. Jain, *Physiol. Rev.,* 2011, **91**, 1071-1121.

17. N. Gligorijevic, S. Arandelovic, L. Filipovic, K. Jakovljevic, R. Jankovic, S. Grguric-Sipka, I. Ivanovic, S. Radulovic, Z. L. Tesic, *J. Inorg. Biochem.,* 2012, **108**, 53-61.

18. C. Kieda, B. Hafny-Rahbi, G. Collet, N. Lamerant-Fayel, C. Grillon, A. Guichard, J. Dulak, A. Jozkowicz, J. Kotlinowski, K. C. Fylaktakidou, A. Vidal, P. Auzeloux, E. Miot-Noirault, B. J. C., J. M. Lehn, C. Nicolau, *J. Mol. Med.,* 2013.

19. G. S. Smith, B. Therrien, *Dalton Trans.,* 2011, **40**, 10793-10800.

20. M. F. Leber, T. Efferth, *Int. J. Oncol.,* 2009, **34**, 881-895.

21. C. Kieda, M. Paprocka, A. Krawczenko, P. Zalecki, P. Dupuis, M. Monsigny, C. Radzikowski, D. Dus, *Endothelium,* 2002, **9**, 247-261.

22. M. Paprocka, A. Krawczenko, D. Dus, A. Kantor, A. Carreau, C. Grillon, C. Kieda, *Cytom. Part A,* 2011, **79A**, 594-602.

23. L. Q. Hu, C. Z. Yu, Y. Y. Jiang, J. Y. Han, Z. R. Li, P. Browne, P. R. Race, R. J. Knox, P. F. Searle, E. I. Hyde, *J. Med. Chem.,* 2003, **46**, 4818-4821.

24. A. Bujak, W. Kalas, *Postep. Hig. Med. Dosw.,* 2008, **62**, 364-371.

Metallomics Accepted Manuscript

25. K. Okuda, Y. Okabe, T. Kadonosono, T. Ueno, B. G. M. Youssif, S. Kizaka-Kondoh, H. Nagasawa, *Bioconjgate Chem.,* 2012, **23**, 324-329.

26. C. A. Puckett, J. K. Barton, *Biochemistry,* 2008, **47**, 11711–11716.

27. E. D. Schwoebel, T. H. Ho, M. S. Moore, *JCB,* 2002, **157**, 963 - 974.

28. E. Reaven, L. Tsai, S. Azhar, *J. Biol. Chem.,* 1996, **271**, 16208-16217.

29. C. A. Puckett, J. R. Ernst, J. K. Barton, *Dalton Trans.,* 2010, **39**, 1159 - 1170.

30. M. Winiarska, J. Bil, E. Wilczek, G. M. Wilczynski, M. Lekka, P. J. Engelberts, W. J. M. Wendy J. M. Mackus, E. Gorska, L. Bojarski, T. Stoklosa, D. Nowis, Z. Kurzaj, M. Makowski, E. Glodkowska, T. Issat, P. Mrowka, W. Lasek, A. Dabrowska-Iwanicka, G. W. Basak, M. Wasik, K. Warzocha, M. Sinski, Z. Gaciong, M. Jakobisiak, P. W. H. I. Parren, J. Golab, *PLOS,* 2008, **5**, 0502-0517.

31. C. A. Lopez, A. H. Vries, S. J. Marrink, *PLOS,* 2011, **7**, 1-11.

32. S. K. Rodal, G. Skretting, O. Garred, F. Vilhardt, B. van Deurs, K. Sandvig, *Mol. Biol. Cell,* 1999, **10**, 961-974.

33. S. Grimmer, B. van Deurs, K. Sandvig, *J. Cell Sci.,* 2002, **115**, 2953-2962.

34. D. A. Kelkar, A. Chattopadhyay, *Biochim. Biophys. Acta,* 2007, **1768**, 2011-2025.

35. M. J. Jaroszeski, R. Heller, *Methods in molecular biology: flow cytometry protocols*. Humana Press: Totowa, N.J, 1997; Vol. 91, p 324.

36. C. A. Puckett, J. K. Barton, *Bioorg. Med. Chem.,* 2010, **18**, 3564-3569.

37. I. V. Tetko, J. Gasteiger, R. Todeschini, A. Mauri, D. Livingstone, P. Ertl, V. A. Palyulin, E. V. Radchenko, N. S. Zefirov, A. S. Makarenko, V. Y. Tanchuk, V. V. Prokopenko, *J. Comput. Aid. Mol. Des.,* 2005, **19**, 453-463.

38. F. R. Svensson, J. Andersson, H. L. Amand, P. Lincoln, *J. Biol. Inorg. Chem.,* 2012, **17**, 565-571.

39. Y. Y. Xie, Z. Z. Li, G. J. Lin, H. L. Huang, X. Z. Wang, Z. H. Liang, G. B. Jiang, Y. J. Liu, *Inorg. Chim. Acta,* 2013, **405**, 228-234.

40. C. A. Lopez, A. H. Vries, S. J. Marrink, *PLOS,* 2011, **7**, 1-11.

41. Y. Chen, B. Lu, Q. Yang, C. Fearns, J. Yates, J. D. Lee, *Cancer Res.,* 2009, **69**, 3713-3720.

42. P. Vaupel, A. Mayer, *Cancer Metastasis Rev.,* 2007, **26**, 225-239.

43. P. Smolewski, Z. Darzynkiewicz, *Acta Haematol. Pol.,* 2003, **4**, 35-47.

44. R. Simantov, R. L. Silverstein, *Front. Biosci.,* 2003, **8**, S874-S882.

45. S. A. Brooks, H. J. Lomax-Browne, T. M. Carter, C. E. Kinch, D. M. S. Hall, *Acta Histochem.,* 2010, **112**, 3-25.

Metallomics Accepted Manuscript

46. S. Wolf, *Jpn. J. Ophthalmol.,* 2008, **52**, 433-439.

47. F. Shojaei, N. Ferrara, *Lab. Invest.,* 2007, **87**, 227-230.

48. S. Lien, H. B. Lowman, *Handbook Exp. Pharmacol.,* 2008, 131-50.

49. J. Weyermann, D. Lochmann, Z. A., *Int. J. Pharm.,* 2005, **288**, 369-376.

50. G. Sava, F. Frausin, M. Cocchietto, F. Vita, E. Podda, P. Spessotto, A. Furlani, V. Scarcia, G. Zabucchi, *Eur. J. Cancer,* 2004, **40**, 1383-1396.

51. C. Tan, S. Hu, J. Liu, L. Ji, *Eur. J. Med. Chem.,* 2011, **46**, 1555-1563.

52. T. Nhukeaw, P. Temboot, K. Hansongnern, A. Ratanaphan, *BMC Cancer,* 2014, **14**.

Metallomics Accepted Manuscript